

The Role of Monocytes/Macrophages In The Pathogenesis of Immune Associated Diffuse Alveolar Hemorrhage

Qing Wei

First Affiliated Hospital of GuangXi Medical University

Xun Chen

First Affiliated Hospital of GuangXi Medical University

Jing Liu

First Affiliated Hospital of GuangXi Medical University

Yan Li

First Affiliated Hospital of GuangXi Medical University

Guangmin Nong (✉ ngm8525@126.com)

First Affiliated Hospital of GuangXi Medical University

Research Article

Keywords: immune associated, diffuse alveolar hemorrhage, monocyte, macrophage, polarization, pathogenesis

Posted Date: May 27th, 2021

DOI: <https://doi.org/10.21203/rs.3.rs-521383/v1>

License:   This work is licensed under a Creative Commons Attribution 4.0 International License.

[Read Full License](#)

Abstract

Background The studies in the immune associated diffuse alveolar hemorrhage (DAH) animal models showed that monocytes/macrophages played an critical role in the pathogenesis. Whether monocytes/macrophages contribute to the pathogenesis of immune associated DAH in human is still unknown. The aim of this study was to explore the role of monocytes/macrophages in the pathogenesis of immune associated DAH in human.

Methods This study was conducted in two parts. In the first part, 37 children with immune associated DAH were included (DAH group), and 18 healthy children were recruited as the controls (HC group). Peripheral blood monocyte subtype was analyzed using flow cytometry. In the second part, 24 children with immune associated DAH were included (DAH group), and 13 children with acute airway foreign body or mild benign airway stenosis were included as the controls (HC group). Bronchoalveolar lavage fluid (BALF) was collected using bronchoscope. Cytokines in the BALF supernatant were detected using cytometric bead array. BALF supernatant was used to stimulate the macrophages in vitro. The mRNA relative expressions of IL-1 β , TNF α , IL-6, TGM2, CD163 and MRC1 were detected using quantitative real-time PCR, and the expressions of CD14, CD80, CD86, CD163 and CD206 were detected using flow cytometry.

Results 1. The percentage of classical monocyte was significantly increased, whereas the percentages of intermediate and non-classical monocyte were significantly decreased in the DAH group, when compared to those in the HC group. 2. The levels of MCP-1, IL-6 and IL-8 were all significantly higher in the BALF supernatant from the DAH group, when compared to those from the HC group. 3. The mRNA relative expressions of IL-1 β and IL-6 as well as the expression of CD86 were significantly higher, whereas the mRNA relative expression of MRC1 as well as the expressions of CD163 and CD206 were significantly lower under the stimulation of BALF supernatant from the DAH group, when compared to that from the HC group.

Conclusions Monocytes/macrophages might participate in the pathogenesis of immune associated DAH in human by enhanced M₁ polarization.

Background

DAH is a severe life-threatening clinical syndrome, and can be caused by a wide variety of etiologies^[1]. Usually, the cases caused by the immune disorders were named immune associated DAH^[1-6]. Until now, the exact pathogenesis of immune associated DAH hasn't been fully understood. Pristane induced DAH murine model has been widely recognised as the immune associated DAH animal model internationally^[7-12]. The studies in the pristane induced murine DAH models have showed that the bone marrow derived monocytes/macrophages in the lungs were the critical factors for developing alveolar hemorrhage, and the enhanced M₁ polarization of the monocytes/macrophages was the key immunological mechanism^[7-12]. Besides the local inflammation in the lungs, systemic inflammation

also participated in the pathogenesis of alveolar hemorrhage, as the monocytes from the bone marrow presented lower expression of IL-10R, whereas the activation of IL-10/IL-10R signalling pathway was found to be a protective factor for developing DAH in the pristane induced murine DAH model^[10]. Whereas, whether monocytes/macrophages contribute to the pathogenesis of immune associated DAH in human remains to be investigated. The purpose of this study was to investigate the role of monocytes/macrophages in the pathogenesis of immune associated DAH in human. In the present study, we found that the peripheral blood classical monocytes were significantly increased, and could be strongly recruited to the lungs in the immune associated DAH. Also, we found that the pulmonary immune microenvironment in the immune associated DAH preferred a pro-inflammatory phenotype, and could promote the M₁ polarization. Taken together, the monocytes/macrophages might be involved in the pathogenesis in the immune associated DAH, and the enhanced M₁ monocytes/macrophage polarization in the lungs might be the key immunological mechanism.

Materials And Methods

Subjects

The study was conducted in two parts. In the first part, total 37 children with immune associated DAH were included, in which 16 cases were classified as the exacerbation group with acute alveolar hemorrhage (DAH-A group), and 21 cases were classified as the remission group without acute alveolar hemorrhage (DAH-R group). And, 18 healthy children were included as the healthy control group (HC group). In the second part, total 24 children with immune associated DAH were included in this study (DAH group). And, 13 children with acute airway foreign body or mild benign airway stenosis, but without infection were included as the control group (HC group). Acute airway foreign body was defined as the time elapsed between aspiration event and foreign body removal within 24 hours. All the subjects with acute airway foreign body included in the control group were absence of any previous health problems, and all the subjects with mild benign airway stenosis were absence of any other previous health problems except the airway stenosis. The subjects with immune associated DAH, and those with acute airway foreign body or mild benign airway stenosis were recruited from the pediatric department of the First Affiliated Hospital of Guangxi Medical University (Nanning, Guangxi, China). The healthy children were recruited from the preventive care department of the same hospital. All the subjects were given informed consent prior to their inclusion in the study. The study was approved by the institutional ethics review board of the First Affiliated Hospital of Guangxi Medical University.

Diagnostic criteria for immune associated DAH and definition of the disease phase

Diagnosis of DAH was based on respiratory symptoms (including dyspnea, hemoptysis and cough), iron deficiency anemia, diffuse pulmonary infiltrates (ground-glass opacities or consolidations) on the chest CT and the presence of hemosiderin laden macrophages in the BALF or lung tissue specimens^[1, 3]. The cases satisfying the above DAH diagnostic criteria, and accompanying with at least one of the following conditions: immune disorders which could result in DAH definitely, pulmonary capillaritis, deposition of

immune substances in the basement membranes of alveolar walls, a good response to immunosuppressive therapy (for the cases without a proven immunological origin, and having excluded the non-immune mediated DAH pathogenic factors) were identified as immune associated DAH^[2-4, 6, 13-16]. A good response to immunosuppressive therapy was defined as relief of respiratory symptoms (dyspnea, hemoptysis), anemia and reduction of pulmonary infiltrates on the chest image within 4-8 weeks of glucocorticoid (prednisone 1-2mg/kg-d or equivalent dose of methylprednisolone) monotherapy or combined with immunosuppressive agents initiation^[5, 17]. Exacerbation phase with acute alveolar hemorrhage was defined as presence of anemia and diffuse pulmonary infiltrates on the chest CT^[15, 18-20]. Remission phase without acute alveolar hemorrhage was defined as absence of hemoptysis, anemia, or pulmonary infiltrates on the chest CT^[15, 18-20].

Bronchoalveolar lavage (BAL) with bronchoscope and BALF processing

Via the bronchoscope, BAL was performed by instilling 10-20 ml of saline into the target segment, with a dwell time of 30 seconds, followed by aspiration. For the children with immune associated DAH, the choice of target segment preferentially selected the medial or lateral segment of the right middle lobe, or the left lingular segment, or the segment with the most obvious pulmonary infiltrates on the chest CT. For the controls, the choice of target segment selected the segment with normal appearance on the chest CT, and preferentially selected the medial or lateral segment of the right middle lobe, or the left lingular segment. To reduce the pollution of bronchial secretions, the BALF from the first lavage was discarded. To obtain the qualified BALF, the BALF recovery rate with greater than 40% was required in this study. Then, the BALF was centrifuged at 2000rpm for 10 min. The supernatant was aspirated and stored at -80°C for soluble proteins assays and cell experiment in vitro.

Detection of the cytokines in the BALF using CBA method

Briefly, 50 µl of BALF supernatant was used to measure the levels of IL-1β, IL-2, IL-5, IL-6, IL-7, IL-8, IL-9, IL-10, IL-13, IL-17A, MCP-1, RANTES, GM-CSF, VEGF, Granzyme B and TNF. Cytokines levels were measured using a CBA kit (BD Bioscience, CA, USA). All experimental procedures were conducted according to the manufacturer's guidelines.

Monocytes isolation and MDMs preparation

Based on the previous studies^[21], peripheral blood was obtained from non-smoking healthy donors. Peripheral blood mononuclear cells (PBMCs) were isolated from EDTA anticoagulant whole blood by FicollPaque (STEMCELL) density gradient centrifugation. PBMCs were suspended in serum-free RPMI 1640 medium (Gibco) supplemented with 100 U/ml penicillin and 100 µg/ml streptomycin (Solarbio), and were seeded in the 6-well (for qRT-PCR) or 12-well (for FCM) culture plate at a density of $1-1.5 \times 10^7$ cells per well for 1-1.5 hours in a humidified incubator containing 5% CO₂ at 37°C to allow monocyte adhesion. Non-adherent cells were removed. The adherent monocytes were further incubated in RPMI 1640 medium (Gibco) supplemented with 10% (v/v) heat-inactivated fetal calf serum (Gibco), 100 U/ml

penicillin and 100 mg/ml streptomycin (Solarbio), and M-CSF (20ng/ml, Sigma-Aldrich) for 7 days with media replacement every 2-3 days to obtain MDMs.

Stimulation of MDMs by BALF supernatant

After 7 days incubation, MDMs were obtained and the medium was replaced with RPMI 1640 medium (Gibco) supplemented with 10% (v/v) heat-inactivated fetal calf serum (Gibco), 100 U/ml penicillin and 100 mg/ml streptomycin (Solarbio), but without M-CSF. Medium was supplemented with 10% (v/v) of subject's BALF supernatant for macrophage stimulation.

RNA purification and qRT-PCR analysis

Twenty-four hours post-stimulation, total RNA of the MDMs was extracted using the AxyPrep Multisource Total RNA Miniprep Kit (Axygen) according to the manufacturer's protocol. Up to 500ng of the total RNA was reverse transcribed using the PrimeScript™ RT reagent kit (Takara) according to the manufacturer's instructions. qRT-PCR reactions were performed using the SYBR Premix Ex Taq II (Tli RNaseH Plus) kit (Takara) with specific primers and run using 7500 Real Time PCR System (Applied Biosystems). All primers were used in the synthesis (Sangon Biotech) and sequences are listed in Table 1. The amount of mRNA was quantified using the $2^{-\Delta\Delta C_t}$ method.

Table 1 PCR primer sequences in this study for the target genes

Gene	Forward	Reverse
IL-1 β	GACCTGGACCTCTGCCCTCTG	GCCTGCCTGAAGCCCTTGC
TNF- α	CGTGGAGCTGGCCGAGGAG	GCAGGCAGAAGAGCGTG GTG
MRC1	GCCAGGGTGTGTTGCCATGAG	TCGGTGGGTGGGTTACTCCTTC
TGM2	TGAGGAGCAGAAGACGGTGGAG	TGTGGAGCGGCAGCAGGTC
CD163	ATCAACCCTGCATCTTTAGACA	CTTGTTGTCACATGTGATCCAG
IL-6	CACTGGTCTTTTGGAGTTTGAG	GGACTTTTGTACTCATCTGCAC

FCM for the peripheral blood monocytes subtype

EDTA anticoagulant blood sample was obtained. Then, 100ul of the EDTA anticoagulant blood was added to the flow tube. Fc receptors (FcR) were blocked using human BD Fc Block™ (BD Biosciences). The cells were stained with PE Mouse Anti-Human CD14 (BD Biosciences) and PE-Cy™7 Mouse Anti-Human CD16(BD Biosciences) for 30 min at 4°C in the dark. Next, erythrocytes were lysed by BD Pharm Lyse™ Lysing Buffer (BD Biosciences). Sample was washed once in PBS before performing FCM.

FCM for the MDMs polarization

After 48h incubation, the *supernatant* was removed, and the cells were washed three times with PBS. Then, the cells were incubated with 1ml 5 mM EDTA (Solarbio) on ice for 20 minutes. Next, the cells were detached by gentle scraping with cell scrapers. After detachment, the cells were washed 2 times with PBS, and were resuspended in 100ul PBS in the flow tube. Fc receptors (FcR) were blocked using human BD Fc Block™ (BD Biosciences). The cells were stained with PE Mouse Anti-Human CD14 (BD Biosciences), PE-Cy™7 Mouse Anti-Human CD80 (BD Biosciences), FITC Mouse Anti-Human CD86 (BD Biosciences), Alexa Fluor® 647 Mouse Anti-Human CD163 (BD Biosciences) and BB700 Mouse Anti-Human CD206 (BD Biosciences) for 30 min at 4°C in the dark. Sample was washed once in PBS before performing FCM. Fluorescence was measured with the FACS Canto II (BD Biosciences). The proportion of cells and the mean fluorescence intensity (MFI) of the markers was determined using FlowJo 7.6 (TreeStar, Ashland, OR).

Statistical analysis

Statistical analysis was performed using SPSS 20.0 soft. Test for normality was performed using the one - sample kolmogorov - smirnov test. The homogeneity of variance test was performed using the Levene's test. For two groups, two - sample t - test was used if the data met normal distribution and variance homogeneity; otherwise, Mann-Whitney U test was used. For multiple groups, one - way ANOVA test followed by post hoc test using the least significance difference test was used if the data met normal distribution and variances homogeneity, if not, by Kruskal - Wallis H test. For the categorical variables, comparisons between groups were performed by the χ^2 test or the Fisher exact test. A two-sided P value \leq 0.05 was considered to be statistically significant.

Results

1. Peripheral blood monocytes subtype in the immune associated DAH

The percentage of classical monocytes was significantly increased ($P \leq 0.01$), and the percentages of intermediate monocytes as well as non-classical monocytes were both significantly decreased (both $P \leq 0.01$) in the DAH-A group, when compared to those in the HC group. The percentage of non-classical monocytes was significantly increased ($P \leq 0.01$) in the DAH-R group, when compared to that in the DAH-A group. The percentage of classical monocytes presented a decreased tendency, and the percentage of intermediate monocytes presented an increased tendency in the DAH-R group, when compared to those in the DAH-A group. However, neither of them had significant differences (both $P > 0.05$). Data are detailed in Table 2 and Figure 1.

Table 2 Comparison of monocyte subtypes from peripheral blood samples among the different groups

Group	N	Classical monocytes (%)	Intermediate monocytes (%)	Non-classical monocytes (%)
DAH	37	93.62±2.53**	4.42±1.92**	1.97±1.27**
DAH-A	16	94.54±2.51**	4.36±2.15**	1.10±0.59**
DAH-R	21	92.93±2.36**	4.47±1.78**	2.63±1.26* ##
HC	18	89.68±2.71	6.89±2.47	3.43±1.01
F_1 value		0.006	1.069	0.961
P_1 value		0.000	0.000	0.000
F_2 value		16.639	8.108	22.316
P_2 value		0.000	0.001	0.000

F_1 , P_1 , DAH group versus HC group, comparisons were performed using two - sample t - test; F_2 , P_2 , DAH-A group versus DAH-r group versus HC group, comparisons were performed using one - way ANOVA test followed by post hoc test using the least significance difference test;

** $P \leq 0.05$, ** $P \leq 0.01$ versus HC group; ## $P \leq 0.01$ versus DAH-A group.

HC, healthy controls; DAH, immune associated DAH; DAH-A, the exacerbation phase with acute alveolar hemorrhage; DAH-R, the remission phase without acute alveolar hemorrhage;

2. Cytokines in the supernatant of BALF

The levels of MCP-1, IL-6 and IL-8 were all significantly higher in the BALF supernatant from the DAH group, when compared to those from the HC group (all $P \leq 0.01$). It was noteworthy that the level of MCP-1 in the BALF supernatant rose most sharply, with nearly 30 folds increase. The levels of IL-2 and IL-9 were both significantly lower in the BALF supernatant from the DAH group, when compared to those from the HC group (with $P \leq 0.05$ and $P \leq 0.01$, respectively). Whereas, there were no significant differences ($P \leq 0.05$) in the levels of IL-1 β , IL-7, IL-10, IL-13, IL-17A, RANTES, GM-CSF, VEGF, Granzyme B or TNF in the BALF supernatant from the DAH group and those from the HC group. The levels of IL-5 were both under the detection threshold in the BALF supernatant from the DAH group and that from HC group. Data are detailed in Table 3.

Table 3 Cytokines in the supernatant of BALF using cytometric bead array

Cytokines (pg/ml)	HC group (N=12)	DAH group (N=24)	<i>F value</i> or <i>Z value</i>	<i>P value</i>
IL-1 β	8.16 \pm 5.73	10.44 \pm 7.41	0.201	0.356
IL-2	6.43 \pm 0.54	6.02 \pm 0.45	1.191	0.020
IL-5	_c	_c	-	-
IL-6 ^a	7.40 \pm 3.82	20.17 \pm 16.00	-3.591 ^d	0.000
IL-7	7.67 \pm 0.77	7.30 \pm 0.85	0.046	0.218
IL-8 ^a	97.92 \pm 79.37	421.17 \pm 422.68	-3.054 ^d	0.002
IL-9	2.73 \pm 0.34	2.26 \pm 0.50	1.006	0.006
IL-10	1.51 \pm 0.45	1.38 \pm 0.36	0.006	0.360
IL-13	3.26 \pm 0.41	3.14 \pm 0.51	0.000	0.507
IL-17A	3.35 \pm 0.51	2.93 \pm 0.66	1.591	0.063
TNF	2.02 \pm 0.34	2.00 \pm 0.49	2.341	0.881
RANTES	89.46 \pm 109.52	131.35 \pm 104.27	0.198	0.272
GM-CSF ^a	1.33 \pm 0.09	1.30 \pm 0.21	-0.807 ^d	0.420
VEGF	148.39 \pm 111.26	121.94 \pm 84.37	0.214	0.431
Granzyme B	27.88 \pm 48.56	22.03 \pm 19.76	2.495	0.609
MCP-1 ^b	45.07 [30.12-81.94]	1234.60 [466.86-2385.12]	-4.564 ^d	0.000

^a The datas could not obtain homogeneity of variance, and were compared using Mann - Whitney U test^b The datas were not normally distributed, and were expressed as median (P 25, P75) and compared using Mann - Whitney U test; The rest datas were expressed as means \pm standard deviation, and compared with two - sample *t* – test; ^c The levels of IL-5 were both under the detection threshold in the BALF supernatant from the DAH group and that from HC group.

^d *Z value*;

DAH, immune associated DAH; HC, Controls.

3. The effect of the supernatant of BALF on the macophage polarization

The mRNA relative expression of IL-1 β and IL-6 were significantly higher (both $P \leq 0.05$), and the mRNA relative expression of MRC1 was significantly lower ($P \leq 0.01$) under the stimulation of BALF supernatant from the DAH group, when compared to those under the stimulation of BALF supernatant from the HC group. Whereas, there was no significant difference in the mRNA relative expression of TNF α , TGM2 or CD163 between the two groups ($P \geq 0.05$). The expression of CD86 was significantly higher ($P \leq 0.05$), and the expressions of CD163 and CD206 were significantly lower (both $P \leq 0.05$) under the stimulation of BALF supernatant from the DAH group, when compared to those under the stimulation of BALF supernatant from the HC group. Whereas, there was no significant difference in the expressions of CD14 and CD80 between the two groups ($P \geq 0.05$). Data are detailed in Table 4, Table 5 and Figure 2.

Table 4 The target genes' relative quantity of mRNA expression in the MDMs when stimulated by BALF supernatant

Group	N	IL-1 β	IL-6	MRC1	TGM2	CD163 ^a	TNF α
DAH	18	5.15 \pm 3.01	38.53 \pm 20.09	0.62 \pm 0.24	1.31 \pm 0.43	20.32 \pm 19.05	7.11 \pm 3.01
HC	13	2.91 \pm 1.14	21.48 \pm 18.48	1.01 \pm 0.48	1.16 \pm 0.45	53.46 \pm 64.59	6.41 \pm 3.66
<i>F value</i> or <i>Z value</i>		3.896	.079	4.144	.077	-0.841 ^b	.180
<i>P value</i>		0.017	0.023	0.006	0.354	0.401	0.563

The datas were expressed as means \pm standard deviation; ^a The datas could not obtain homogeneity of variance, and were compared using Mann - Whitney U test; The rest datas were compared with two - sample *t* - test.

^b *Z value*;

DAH, Immune associated DAH; HC, Controls.

Table 5 The expression of the CD14, CD80, CD86, CD163 and CD206 on the surface of MDMs when stimulated by BALF supernatant

Group	N	CD14 positive rate(%)	CD80 positive rate(%)	CD86 positive rate(%)	CD163 positive rate(%)	CD206 ^a (MFI)
DAH	18	83.22±8.34	58.85±10.34	25.09±11.19	36.88±12.99	1226.72±413.11
HC	12	88.63±5.62	60.24±8.42	17.40±7.82	52.25±15.39	1821.83±888.88
<i>F value or Z value</i>		1.758	.276	.000	.571	-2.074 ^b
<i>P value</i>		0.06	0.701	0.049	0.016	0.038

The datas were expressed as means ± standard deviation; ^a The datas could not obtain homogeneity of variance, and were compared using Mann - Whitney U test; The rest datas were compared with two - sample *t* - test.

^b *Z value*;

DAH, Immune associated DAH; HC, Controls; MFI, mean fluorescence index.

Discussion

The classification of DAH as “immune mediated” and “non-immune mediated” was first proposed by Tobias Peikert in 2012^[2]. In the Tobias Peikert’s classification system, the DAH cases accompanying with autoimmune disorders (such as SLE, AAV, Goodpasture disease) or pulmonary capillaritis were defined as immune mediated DAH^[2]. However, this classification system had some limitations. In recent, immune disorders caused by gene mutation, such as COPA syndrome and STING-associated vasculopathy with onset in infancy (SAVI) were found to develop DAH^[22, 23]. SpC dysfunction with the I73T mutation was also found to develop autoimmunity accompanying with DAH^[24]. Besides that, the DAH cases who had excluded the non-immune mediated pathogenic factors should be highly suspected for immune mediated either, in which some were found to had pulmonary capillaritis^[25] or deposition of immune substances in the basement membranes of alveolar walls in the lung biopsy^[26], some were found to be the autoimmune diseases or develop autoantibodies during the follow-up^[27, 28], and some cases were the idiopathic pulmonary hemosiderosis (IPH). IPH was classified as the non-immune mediated DAH in the Tobias Peikert’s classification system, as there was no pulmonary capillaritis or autoantibody in the IPH. However, a considerable number of relevant studies have found that IPH presented a good response to immunosuppressive therapy, which indicated that IPH was also immune mediated^[1, 3, 6, 29]. Referring to the Tobias Peikert’s classification system and the recent research advances mentioned above, we reconceptualized the immune mediated DAH. To avoid confusion with Tobias Peikert’s classification system, the DAH cases included in this study were named “immune associated DAH” instead of “immune mediated DAH”.

Recently, the studies in the pristane induced murine DAH models have demonstrated that the bone marrow derived monocytes/macrophages in the lungs were the critical factors for developing alveolar hemorrhage, and the enhances M₁ polarization of the monocytes/macrophages was the key immunological mechanism. Besides the local inflammation in the lungs, systemic inflammation also participated in the pathogenesis of alveolar hemorrhage, as the monocytes from the bone marrow in the pristane induced murine DAH model presented lower expression of IL-10R. Whereas, whether monocytes/macrophages contribute to the pathogenesis of immune associated DAH in human remains to be investigated. In view of this, we conducted this study to investigate the role of monocytes/macrophages in the pathogenesis of immune associated DAH in human.

According to the expression of CD14 and CD16, the peripheral blood monocytes were classified as classical (CD14⁺⁺/CD16⁻), intermediate (CD14⁺⁺ /CD16⁺) and non-classical (CD14⁺ /CD16⁺⁺) monocytes^[30]. Classical monocytes could migrate into the tissue, and initiate or regulate the inflammatory response^[30, 31]. Whereas, non-classical monocytes usually displayed a distinct motility and crawling pattern along the vasculature to survey the luminal side of vascular endothelium and maintain the vascular homeostasis^[32]. Intermediate monocytes were considered to be the transition state between the classical and non-classical monocytes^[31]. In this study, we found that the peripheral blood classical monocytes were significantly increased in the children with immune associated DAH, which demonstrated that the peripheral blood monocytes in the immune associated DAH preferred to migrate into the tissue and to be a pro-inflammation phenotype. Also, we found that the abnormalities of the peripheral blood monocytes subtype presented a tendency to normalization with the disease remission, which further suggested that the peripheral blood monocytes participated in the pathogenesis of immune associated DAH.

BALF supernatant contained a large number of soluble immune mediators, and could represent the pulmonary immune microenvironment^[33]. In this study, we found that the levels of MCP-1, IL-6 and IL-8 were all significantly increased in the BALF supernatant from the children with immune associated DAH, in which the level MCP-1 rose most sharply with nearly 30 folds increase. In viro cell experiments, we found that BALF supertanant from the children with immune associated DAH significantly enhanced the mRNA relative expression of IL-1 β as well as IL-6 and the expression of CD86, whereas reduced the mRNA relative expression of MRC1 and the expression of CD163 as well as CD206. According to the literature, MCP-1, IL-6 and IL-8 were all pro-inflammatory mediators^[34-37], and MCP-1 was a potent chemoattractant for monocytes^[38]. Enhanced trancription of IL-1 β as well as IL-6 and expression of CD86, accompanying with reduced trancription of MRC1 and expression of CD163 as well as CD206 were the markers of M₁ polarization^[39-42]. Thus, our results indicated that the pulmomyary immune microenviroment in the immune associated DAH preferred a pro-inflammatory phenotype, which could strongly favored the recruitment of the peripheral blood monocytes, and promote the M₁ polarization. It was noteworthy that this result echoed with our previous finding in which the peripheral blood monocytes in the immune associated DAH preferred to migrate into the tissue and to be a pro-inflammation phenotype. Taken together, the monocytes/macrophages were involved in pathogenesis in the immune

associated DAH, and the enhanced M₁ monocytes/macrophage polarization in the lungs might play a role in the pathogenesis of immune associated DAH.

Type 2 immunity was characterized by the production of IL4, IL5, IL9 and IL13, and was mainly involved in the allergic inflammation, tissue repair after injury and fibrosis^[43]. In this study, we found that the level of IL-9 was significantly reduced, the level of IL-13 revealed no significant difference, and the level of IL-5 was under the detection threshold in the BALF supernatant from the children with immune associated DAH. The result suggested that type 2 immunity was in an inactive state in the pulmonary immune microenvironment of the immune associated DAH. And, it also indicated that type 2 immunity might not participate in the pathogenesis of alveolar hemorrhage. Whereas, recurrent episodes of DAH usually resulted in interstitial fibrosis^[1]. Given the important role of type 2 immunity in the fibrosis, type 2 immunity might participate in the alveolar wall repair process following the damage in the immune associated DAH. A further study on the relation between the type 2 immunity and the interstitial fibrosis in the immune associated DAH should be explored.

Our study had some limitations. Firstly, we didn't enroll the healthy children to perform bronchoalveolar lavage due to ethical restrictions. Whereas, to reduce the selection bias of controls, we had set a strict inclusion criteria, and chosen the segment with normal appearance on the chest CT to perform bronchoalveolar lavage. Secondly, we didn't perform stratified analysis by disease staging in the BALF supernatant part of this study, as the majority of the cases included were in the exacerbation stage. Finally, the number of subjects included in this study was small, and should be expanded in the future.

Conclusions

The monocytes/macrophages might be involved in the pathogenesis in the immune associated DAH, and the enhanced M₁ monocytes/macrophage polarization in the lungs might be the key immunological mechanism.

Abbreviations

DAH: diffuse alveolar hemorrhage; BALF: bronchoalveolar lavage fluid; qRT-PCR: quantitative real-time PCR; FCM: flow cytometry; PBMCs: peripheral blood mononuclear cells; MDMs: monocytes derived macrophages; HC: healthy control; PBMC: peripheral blood mononuclear cell; FcR: Fc receptors; IPH: idiopathic pulmonary hemosiderosis; SLE: systemic lupus erythematosus; AAV: ANCA-associated vasculitis; GD: goodpasture disease. IL: interleukin; MCP-1: monocyte chemoattractant protein-1.

Declarations

Ethics approval and consent to participate

The study was approved by the institutional ethics review board of the First Affiliated Hospital of Guangxi Medical University. A written informed consent was obtained from each study subject or from his/her guardian.

Consent for publication

Not applicable.

Availability of data and materials

We would like to provide the raw data to support the information presented in this publication.

Competing interests

The authors have no conflicts of interest relevant to this article to disclose.

Funding

This study were supported by the grant (principal investigator: Guangmin Nong) from the the First Affiliated Hospital of Guangxi Medical University (YYZS2020014) and the grant (principal investigator: Qing Wei) from Guangxi Medical University (GXMUYSF202114).

Authors' contributions

Q Wei and X Chen took part in designing the study, performed the experiments, carried out the acquisition, analysis as well as the interpretation of the datas, and drafted the manuscript. GM Nong conceptualized and designed the whole study, supervised and instructed data collection and analysis, reviewed and revised the manuscript. J Liu and Y Li contributed to the overall design of the study, performed the bronchoalveolar lavage with bronchoscope, and critically reviewed the manuscript. All authors have read and approved the final manuscript.

Acknowledgements

This study would like to thank the participants who gave their time to contribute to this study.

References

1. Lara AR, Schwarz MI. Diffuse alveolar hemorrhage. *Chest*. 2010;137(5):1164-71.
2. Krause ML, Cartin-Ceba R, Specks U, Peikert T. Update on diffuse alveolar hemorrhage and pulmonary vasculitis. *Immunol Allergy Clin North Am*. 2012;32(4):587-600.
3. Taytard J, Nathan N, de Blic J, Fayon M, Epaud R, Deschildre A, et al. New insights into pediatric idiopathic pulmonary hemosiderosis: the French RespiRare((R)) cohort. *Orphanet J Rare Dis*. 2013;8:161.
4. Quadrelli S, Dubinsky D, Solis M, Yucra D, Hernandez M, Karlen H, et al. Immune diffuse alveolar hemorrhage: Clinical presentation and outcome. *Respir Med*. 2017;129:59-62.

5. Park JA. Treatment of Diffuse Alveolar Hemorrhage: Controlling Inflammation and Obtaining Rapid and Effective Hemostasis. *Int J Mol Sci.* 2021;22(2):793.
6. Saha BK. Idiopathic pulmonary hemosiderosis: A state of the art review. *Respir Med.* 2021;176:106234.
7. Barker TT, Lee PY, Kelly-Scumpia KM, Weinstein JS, Nacionales DC, Kumagai Y, et al. Pathogenic role of B cells in the development of diffuse alveolar hemorrhage induced by pristane. *Lab Invest.* 2011;91(10):1540-50.
8. Shi Y, Tsuboi N, Furuhashi K, Du Q, Horinouchi A, Maeda K, et al. Pristane-induced granulocyte recruitment promotes phenotypic conversion of macrophages and protects against diffuse pulmonary hemorrhage in Mac-1 deficiency. *J Immunol.* 2014;193(10):5129-39.
9. Zhou S, Wang Y, Meng Y, Xiao C, Liu Z, Brohawn P, et al. In Vivo Therapeutic Success of MicroRNA-155 Antagomir in a Mouse Model of Lupus Alveolar Hemorrhage. *Arthritis Rheumatol.* 2016;68(4):953-64.
10. Zhuang H, Han S, Lee PY, Khaybullin R, Shumyak S, Lu L, et al. Pathogenesis of Diffuse Alveolar Hemorrhage in Murine Lupus. *Arthritis Rheumatol.* 2017;69(6):1280-93.
11. Han S, Zhuang H, Shumyak S, Wu J, Xie C, Li H, et al. Liver X Receptor Agonist Therapy Prevents Diffuse Alveolar Hemorrhage in Murine Lupus by Repolarizing Macrophages. *Front Immunol.* 2018;9:135.
12. Lee PY, Nelson-Maney N, Huang Y, Levescot A, Wang Q, Wei K, et al. High-dimensional analysis reveals a pathogenic role of inflammatory monocytes in experimental diffuse alveolar hemorrhage. *JCI Insight.* 2019;4(15) : e129703.
13. Picard C, Cadranel J, Porcher R, Prigent H, Levy P, Fartoukh M, et al. Alveolar haemorrhage in the immunocompetent host: a scale for early diagnosis of an immune cause. *Respiration.* 2010;80(4):313-20.
14. de Prost N, Parrot A, Cuquemelle E, Picard C, Antoine M, Fleury-Feith J, et al. Diffuse alveolar hemorrhage in immunocompetent patients: etiologies and prognosis revisited. *Respir Med.* 2012;106(7):1021-32.
15. de Prost N, Parrot A, Cuquemelle E, Picard C, Cadranel J. Immune diffuse alveolar hemorrhage: a retrospective assessment of a diagnostic scale. *Lung.* 2013;191(5):559-63.
16. Zhang Y, Luo F, Wang N, Song Y, Tao Y. Clinical characteristics and prognosis of idiopathic pulmonary hemosiderosis in pediatric patients. *J Int Med Res.* 2019;47(1):293-302.
17. Saha BK, Milman NT. Idiopathic pulmonary hemosiderosis: a review of the treatments used during the past 30 years and future directions. *Clin Rheumatol.* 2020.
18. Spira D, Wirths S, Skowronski F, Pintoffl J, Kaufmann S, Brodoefel H, et al. Diffuse alveolar hemorrhage in patients with hematological malignancies: HRCT patterns of pulmonary involvement and disease course. *Clin Imaging.* 2013;37(4):680-6.
19. Lichtenberger JP, 3rd, Digumarthy SR, Abbott GF, Shepard JA, Sharma A. Diffuse pulmonary hemorrhage: clues to the diagnosis. *Curr Probl Diagn Radiol.* 2014;43(3):128-39.

20. Sun Y, Zhou C, Zhao J, Wang Q, Xu D, Zhang S, et al. Systemic lupus erythematosus-associated diffuse alveolar hemorrhage: a single-center, matched case-control study in China. *Lupus*. 2020;29(7):795-803.
21. Vogel DY, Glim JE, Stavenuiter AW, Breur M, Heijnen P, Amor S, et al. Human macrophage polarization in vitro: maturation and activation methods compared. *Immunobiology*. 2014;219(9):695-703.
22. Tsui JL, Estrada OA, Deng Z, Wang KM, Law CS, Elicker BM, et al. Analysis of pulmonary features and treatment approaches in the COPA syndrome. *ERJ Open Res*. 2018;4(2) : 00017-2018.
23. Tang X, Xu H, Zhou C, Peng Y, Liu H, Liu J, et al. STING-Associated Vasculopathy with Onset in Infancy in Three Children with New Clinical Aspect and Unsatisfactory Therapeutic Responses to Tofacitinib. *J Clin Immunol*. 2020;40(1):114-22.
24. Tang X, Shen Y, Zhou C, Yang H, Liu H, Li H, et al. Surfactant protein C dysfunction with new clinical insights for diffuse alveolar hemorrhage and autoimmunity. *Pediatr Investig*. 2019;3(4):201-6.
25. Xie J, Zhao YY, Liu J, Nong GM. Diffuse alveolar hemorrhage with histopathologic manifestations of pulmonary capillaritis Three case reports. *World J Clin Cases*. 2020;8(12):2662-6.
26. Buckley M, Van Mater H. Idiopathic Pulmonary Hemosiderosis as a Mimic of Pulmonary Vasculitis: A Case Report and Review of the Literature. *Curr Allergy Asthma Rep*. 2020;20(5):13.
27. Boardman EA, Sohail S, Yadavilli R. Goodpasture's disease with late presentation of renal abnormality and anti-GBM autoantibody. *BMJ Case Rep*. 2017;2017: bcr2016218705.
28. Stainer A, Rice A, Devaraj A, Barnett JL, Donovan J, Kokosi M, et al. Diffuse alveolar haemorrhage associated with subsequent development of ANCA positivity and emphysema in three young adults. *BMC Pulm Med*. 2019;19(1):185.
29. Fullmer JJ, Langston C, Dishop MK, Fan LL. Pulmonary capillaritis in children: a review of eight cases with comparison to other alveolar hemorrhage syndromes. *J Pediatr*. 2005;146(3):376-81.
30. Coillard A, Segura E. In vivo Differentiation of Human Monocytes. *Front Immunol*. 2019;10:1907.
31. Guilliams M, Mildner A, Yona S. Developmental and Functional Heterogeneity of Monocytes. *Immunity*. 2018;49(4):595-613.
32. Narasimhan PB, Marcovecchio P, Hamers AAJ, Hedrick CC. Nonclassical Monocytes in Health and Disease. *Annu Rev Immunol*. 2019;37:439-56.
33. Wattiez R, Falmagne P. Proteomics of bronchoalveolar lavage fluid. *J Chromatogr B Analyt Technol Biomed Life Sci*. 2005;815(1-2):169-78.
34. Hunter CA, Jones SA. IL-6 as a keystone cytokine in health and disease. *Nature Immunology*. 2015;16(5):448-57.
35. Bianconi V, Sahebkar A, Atkin SL, Pirro M. The regulation and importance of monocyte chemoattractant protein-1. *Curr Opin Hematol*. 2018;25(1):44-51.
36. Meniailo ME, Malashchenko VV, Shmarov VA, Gazatova ND, Melashchenko OB, Goncharov AG, et al. Interleukin-8 favors pro-inflammatory activity of human monocytes/macrophages. *Int Immunopharmacol*. 2018;56:217-21.

37. Kany S, Vollrath JT, Relja B. Cytokines in Inflammatory Disease. *Int J Mol Sci.* 2019;20(23).
38. Gschwandtner M, Derler R, Midwood KS. More Than Just Attractive: How CCL2 Influences Myeloid Cell Behavior Beyond Chemotaxis. *Front Immunol.* 2019;10:2759.
39. Roussel M, Ferrell PB, Jr., Greenplate AR, Lhomme F, Le Gallou S, Diggins KE, et al. Mass cytometry deep phenotyping of human mononuclear phagocytes and myeloid-derived suppressor cells from human blood and bone marrow. *J Leukoc Biol.* 2017;102(2):437-47.
40. Shiratori H, Feinweber C, Luckhardt S, Linke B, Resch E, Geisslinger G, et al. THP-1 and human peripheral blood mononuclear cell-derived macrophages differ in their capacity to polarize in vitro. *Mol Immunol.* 2017;88:58-68.
41. Tedesco S, De Majo F, Kim J, Trenti A, Trevisi L, Fadini GP, et al. Convenience versus Biological Significance: Are PMA-Differentiated THP-1 Cells a Reliable Substitute for Blood-Derived Macrophages When Studying in Vitro Polarization? *Front Pharmacol.* 2018;9:71.
42. Ahmed F, Ibrahim A, Cooper CL, Kumar A, Crawley AM. Chronic Hepatitis C Virus Infection Impairs M1 Macrophage Differentiation and Contributes to CD8(+) T-Cell Dysfunction. *Cells.* 2019;8(4).
43. Gieseck RL, 3rd, Wilson MS, Wynn TA. Type 2 immunity in tissue repair and fibrosis. *Nat Rev Immunol.* 2018;18(1):62-76.

Figures

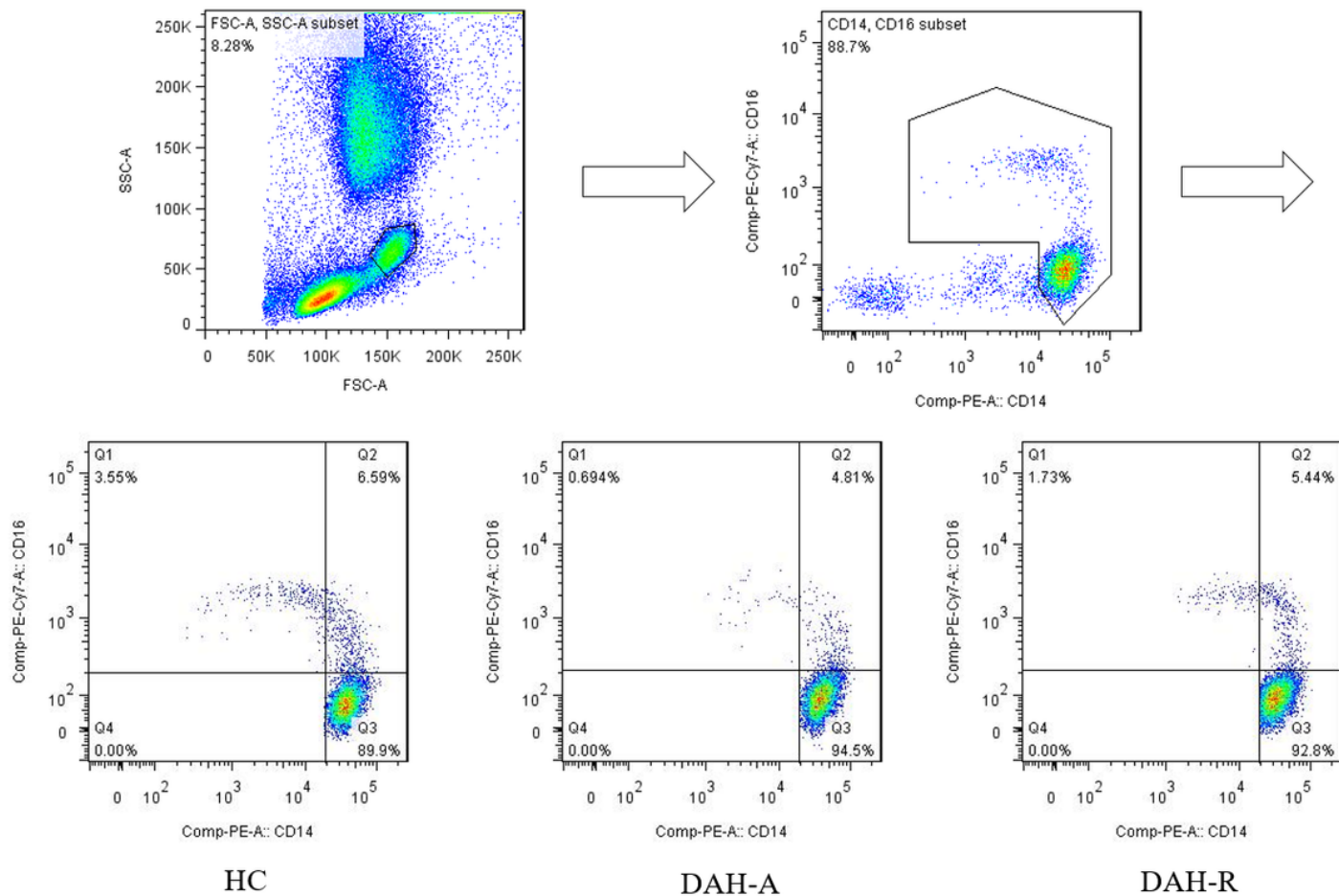


Figure 1

Representative flow cytometric profiles of monocyte subtypes from the peripheral blood

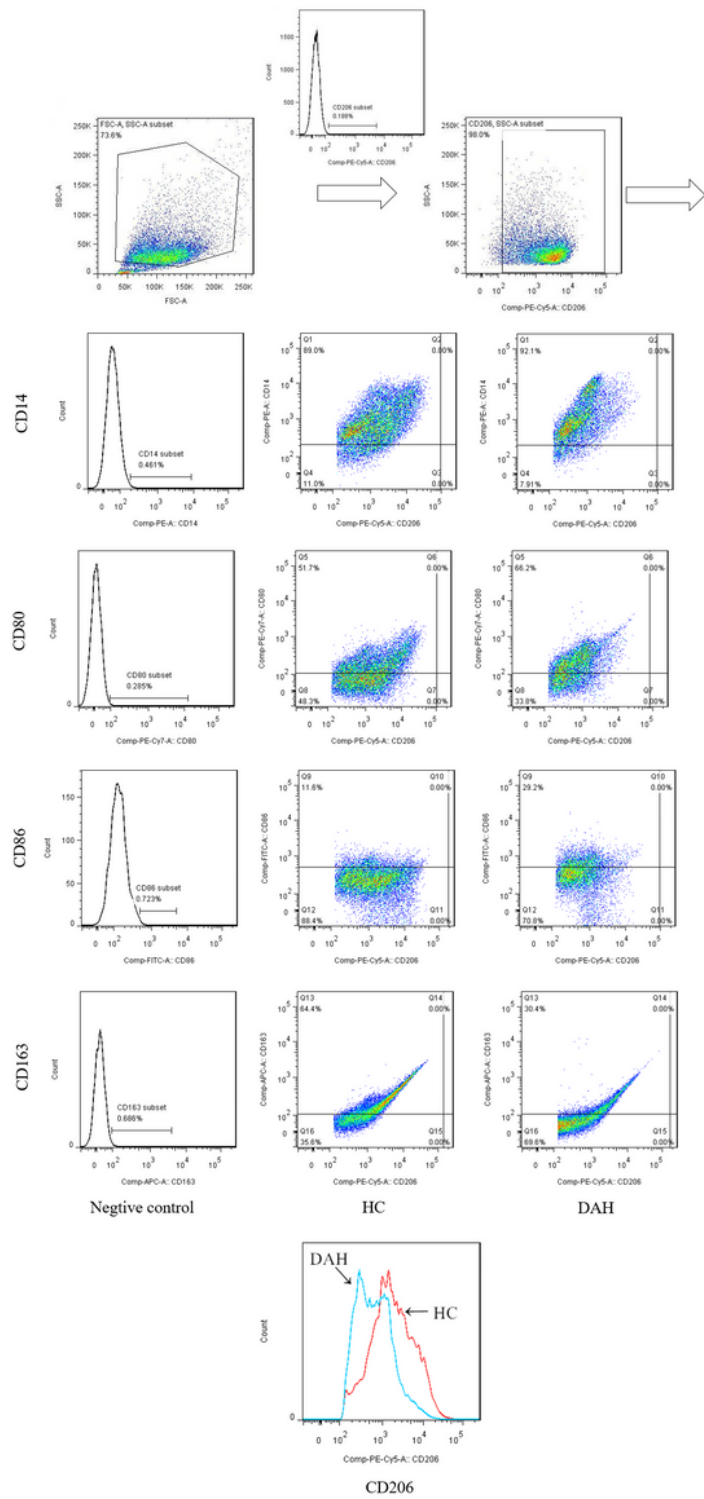


Figure 2

Representative flow cytometric profiles of CD14, CD80, CD86, CD163 and CD206 expression on the surface of MDMs stimulated by the BALF supernatant